Tellus
SERIES A
DYNAMIC
METEOROLOGY
AND OCEANOGRAPHY
PUBLISHED BY THE INTERNATIONAL METEOROLOGICAL INSTITUTE IN STOCKHOLM

Tellus (2009), 61A, 466–475
Printed in Singapore. All rights reserved

TELLUS

The Iceland–Lofotes pressure difference: different states of the North Atlantic low-pressure zone

By ANNIKA JAHNKE-BORNEMANN* and BURGHARD BRÜMMER, *Meteorological Institute, University of Hamburg, D-20146 Hamburg, Germany*

(Manuscript received 28 April 2008; in final form 16 March 2009)

ABSTRACT

The extended North Atlantic low-pressure zone exhibits two pressure minima in the long-term winter mean: the primary one west of Iceland and the secondary one near Norwegian Lofotes Islands. Based on the ERA-40 data set and on wintertime monthly sea level pressure (SLP) anomalies at both places, the states of co- and antivariability are investigated. The covariability represents states of a strongly or weakly developed North Atlantic low-pressure zone. The difference between these two states represents the NAO pattern. The antivariability is defined by an Iceland–Lofotes difference (ILD) index, which is positive (negative) when the anomaly in the Lofotes area is higher (lower) than that in the Iceland area. An ILD pattern is calculated as difference between SLP composites for high and low ILD indices. The ILD pattern extends horizontally beyond the two centers and affects other prominent Northern Hemisphere pressure centres: Aleutian low; Siberian high and Azores high. The pattern extends into the stratosphere and shows significant impacts on surface air temperature, Arctic sea ice concentration and sea ice motion.

1. Introduction

The dominating pattern of pressure variation over the North Atlantic is the North Atlantic oscillation (NAO), whose state and magnitude is given by the NAO index. The NAO index is defined as the normalized pressure difference between Iceland (representing the Icelandic Low) and the Azores, Portugal or south Spain (representing the Azores high) (e.g. Hurrell, 1995; Jones et al., 1997) or by the normalized principal component of the first empirical orthogonal function (EOF) of the North Atlantic pressure field (e.g. Hurrell et al., 2003). The NAO is closely related to the hemispheric mode of variability, the Arctic oscillation (AO) (Wallace, 2000; Ambaum et al., 2001) and accounts for about one third of the total pressure variation. The NAO centres of action, the Icelandic low and the Azores high are not fixed geographically but can undergo shifts in west-east direction (e.g. Rogers, 1997; Ulbrich and Christoph, 1999; Hilmer and Jung, 2000). Changes of the strength and position of the NAO centres mainly cause the wintertime air-temperature variations in Europe and determine the North Atlantic storm track (Rogers, 1997). However, the NAO index is not or only for certain time periods correlated with the air-temperature see-saw between Greenland and northern Europe (Rogers, 1997), the sea ice export variations through Fram Strait (Hilmer and Jung, 2000) or the occurrence of mild Siberian winters (Rogers and Mosley-Thompson, 1995). Quite a few previous studies addressed the NAO and its relationship to the storm track and cyclone behaviour (e.g. Serreze et al., 1997).

In this paper, we concentrate on the elongated North Atlantic low-pressure zone, which is generally referred to as the Icelandic low. However, this is not a precise term because the low-pressure zone extends over a long distance from the Irminger Sea west of Iceland to the Barents Sea (Fig. 1). The mean wintertime (DJF) sea level pressure (SLP) field shows two minima within the low-pressure zone: a primary one over the Irminger Sea and a secondary one near the Norwegian Lofotes Islands. There are variations in the locations of the pressure minima from winter to winter, but the locations predominantly cluster in two areas—a southwestern one and a northeastern one (Fig. 2)—which we refer to as the Iceland (I) area and the Lofotes (L) area, respectively. There is a wide gap between these two cluster areas. The individual winter SLP means show either one pressure minimum (either in the I or L area) or two pressure minima with the absolute pressure minimum either in the I or L area. The frequency statistics of these four states is given in Table 1. Although a minimum in the Iceland area is most frequent, a minimum in the Lofotes area occurs (as primary or secondary minimum) in the North Atlantic low-pressure zone in about 62% of the 45 winter season averages (DJF).

The goal of this paper is to analyse the pressure distribution within the North Atlantic low-pressure zone in more detail and to find out if the variability of the pressure differences between

*Corresponding author.
e-mail: annika.bornemann@zmaw.de
DOI: 10.1111/j.1600-0870.2009.00401.x

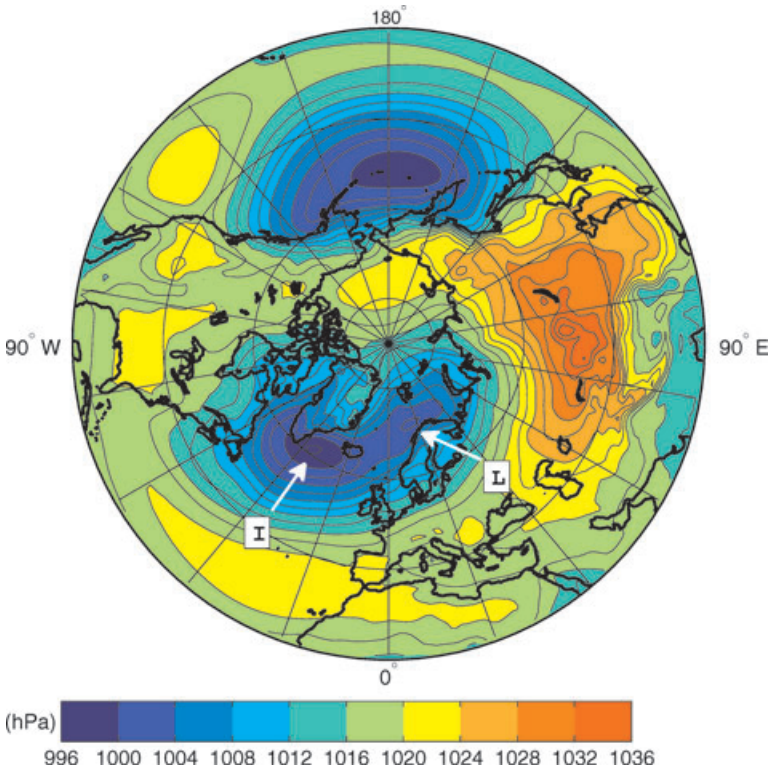

Fig. 1. Mean sea level pressure for winter (DJF) for the ERA-40 period 1957–2002. Labels I and L mark Irminger Sea and Lofotes Islands region, respectively.

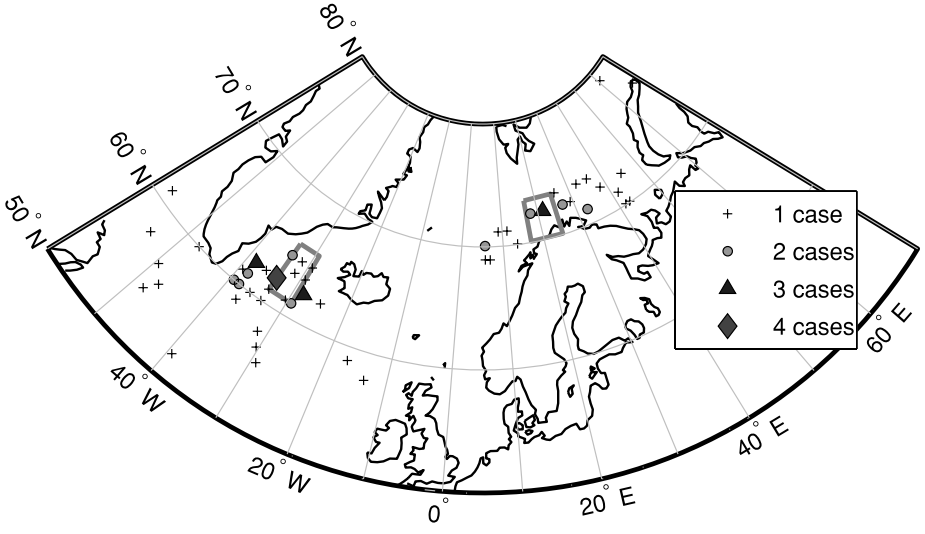

Fig. 2. Locations of SLP minima in the individual 45 winter (DJF) averages for the ERA-40 period 1957–2002. The number of SLP minima is more than 45 because two minima occur in some winters. Boxes indicate sub-areas I and L taken for ILD index calculation.

these two areas, which we name the Iceland–Lofotes difference (ILD), is limited to the North Atlantic low-pressure zone or reaches even further beyond. In Section 2, the data and the methods are presented. We define an Iceland–Lofotes index (ILD index), which describes the pressure difference within the North Atlantic low-pressure zone between the Iceland and Lofotes area. In Section 3, the temporal variability of the ILD index is analysed. Based on high and low index values, we calculate the pressure difference pattern (ILD pattern) between Iceland and Lofotes composites. Since the ILD pattern causes meridional flow variations, it affects the surface air temperature (SAT) over the northeast Atlantic as well as the Arctic sea ice, especially the

Table 1. Absolute and relative frequencies of the location of the North Atlantic SLP minimum in the Iceland region (I), Lofotes region (L) or in case of two minima with the absolute minimum either in the I or L region (underlined) for 45 winter seasons (DJF mean) and 135 winter months (D, J, F means) for the period 1957–2002

	I	I/L	I/L	L
Winter seasons (45)	17 (38%)	16 (36%)	11 (24%)	1 (2%)
Winter months (135)	46 (34%)	52 (39%)	18 (13%)	19 (14%)

sea ice export through Fram Strait. This impact is investigated in Section 4. The paper closes with a discussion of the results in Section 5.

2. Data and methods

For this study, we use the ERA-40 reanalyses (Uppala et al., 2005) provided by the European Centre for Medium-Range Weather Forecasts (ECMWF) for the period 1957–2002. Reanalyses provide consistent and equally gridded data over a long time period and are produced with a fixed model/assimilation system; a limitation is that not the latest operational model system is used. The ERA-40 data set has a horizontal resolution of 1.125°, which is a higher resolution than, for example, that of the National Center for Environmental Prediction (NCEP) reanalysis data. Since we are interested in timescales beyond the synoptic scale, the 6-hourly ERA-40 data fields are averaged to monthly means. To describe the state of SLP distribution within the North Atlantic low-pressure zone, we use the SLP mean in a 5 × 5 gridpoints subarea in the I area and in a 4 × 8 gridpoints subarea of a similar size ($\sim 10^5$ km^2) in the L area (see Fig. 2). The locations of the two subareas are chosen to approximately represent the locations of three observational findings: (1) the two wintertime mean SLP minima in Fig. 1; (2) the centres of the two cluster areas in Fig. 2 and (3) the regions of the primary (Iceland) and the secondary (Lofotes) maximum of cyclone frequency over the North Atlantic (e.g. Affeld, 2003; Wernli and Schwierz, 2006).

Figure 3 represents a scatter diagram of the normalized pressure anomalies for the I area

$$\Delta p_{\mathrm{I}} = (p_{\mathrm{I}}(k) - \bar{p}_{\mathrm{I}})/\sigma_{\mathrm{pI}} \tag{1a}$$

and L area

$$\Delta p_{\mathrm{L}} = (p_{\mathrm{L}}(k) - \bar{p}_{\mathrm{L}})/\sigma_{\mathrm{pL}} \tag{1b}$$

for the 135 winter months. In eqs. (1) p is SLP, k is a running number for the individual months, overbar denotes the 1957–2002 average, σ is standard deviation and indices I, L refer to Iceland or Lofotes, respectively. The standard deviation σ_{pI} is

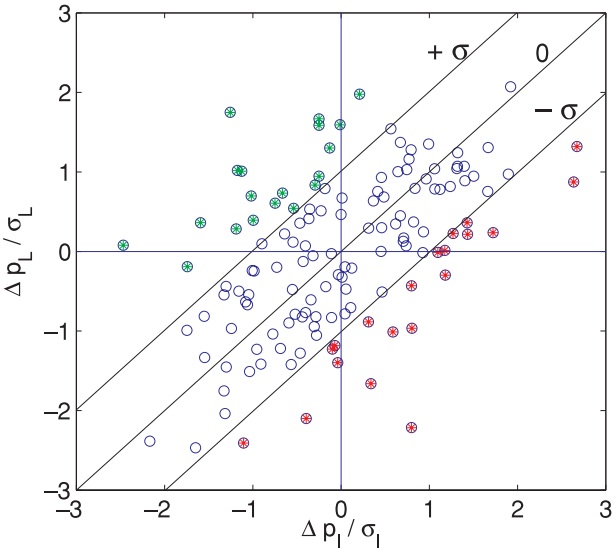

Fig. 3. Scatter plot of normalized (by corresponding standard deviation) SLP anomaly in the Iceland (I) and Lofotes (L) area for 135 winter months (D, J, F) for the ERA-40 period 1957–2002. Green dots above the diagonal (ILD = $+\sigma$) mark months with ILD standard deviation $>+1$, red dots below the diagonal (ILD = $-\sigma$) mark months with ILD standard deviation < -1.

9.0 hPa and σ_{pL} is 7.6 hPa. Both anomalies are simultaneously positive in 47 winter months, simultaneously negative in 46 months and have opposite sign in 42 months.

The SLP difference pattern between the 47 composite cases with $\Delta p_{\mathrm{L}} > 0$ and $\Delta p_{\mathrm{I}} > 0$ minus the 46 composite cases with $\Delta p_{\mathrm{L}} < 0$ and $\Delta p_{\mathrm{I}} < 0$ results in a pattern similar to the NAO pattern (Fig. 4a). The SLP difference pattern between the 16 composite cases with $\Delta p_{\mathrm{L}} < 0$ and $\Delta p_{\mathrm{I}} > 0$ minus the 26 composite cases with $\Delta p_{\mathrm{L}} > 0$ and $\Delta p_{\mathrm{I}} < 0$ (Fig. 4b) yields an east-west pattern (Fig. 4b), which this study focuses on in detail.

In analogy to Hurrell's (1995) definition of the NAO index, we describe the pressure difference between the I area and the L area with an ILD index as follows:

$$\mathrm{ILD} = \Delta p_{\mathrm{L}} - \Delta p_{\mathrm{I}}. \tag{2}$$

The ILD index is positive, if the normalized pressure anomaly in the L area is higher than the normalized pressure anomaly in the I area. Thus, by the definition in (2), one obtains positive and negative ILD values independent of the general pressure level of the North Atlantic low-pressure zone. Composite pressure fields are calculated separately for large positive and large negative ILD indices, and afterwards the two composites are subtracted from each other. The resulting pattern is named ILD pattern. The conditions prescribed for the two composites are that the ILD index is at least one standard deviation (standard deviation of ILD index is $\sigma_{\mathrm{ILD}} = 1.01$) either above or below the mean value. In Fig. 3, the 19 months with positive ILD values and

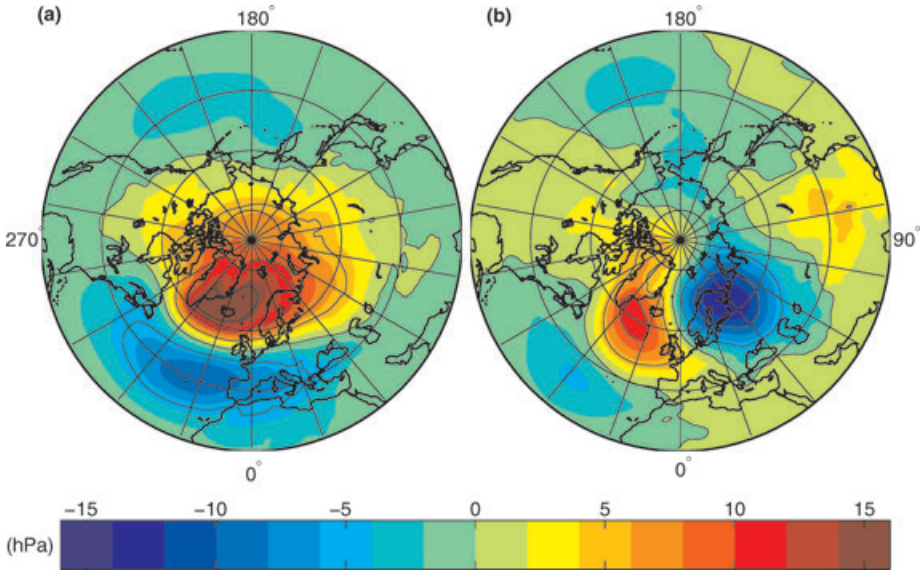

Fig. 4. (a) Difference pattern of SLP composite for positive anomalies in the I and L area minus SLP composite for negative anomalies in the I and L area. (b) Difference pattern of SLP composite for positive anomalies in the I and negative anomalies in the L area minus SLP composite for negative anomalies in the I and positive anomalies in the L area.

the 20 months with negative ILD values larger than the $\pm\sigma_{\mathrm{ILD}}$ criteria are marked.

3. ILD index and pattern

The ILD pattern, that is, the composite SLP field for ILD index less than –1 standard deviation minus the composite SLP field for ILD index more than +1 standard deviation, is presented in Fig. 5. The ILD pattern, based on the more general definition of the Iceland–Lofotes pressure difference in eq. (2), widely resembles the SLP difference pattern in Fig. 4b based on strictly opposite SLP anomalies. In the ILD pattern, two primary centres with opposite pressure difference emerge near the I and L areas. They are located slightly outside of the two gridpoint areas (Fig. 2) that were taken for the ILD index calculation. The southwest centre is located east of the southern tip of Greenland and the northeast centre is located over northeast Scandinavia. The SLP differences connected with the two states of pressure distribution within the North Atlantic low-pressure zone are not restricted to this region but show three further secondary centres like a wave train outside of the region. Interestingly, the locations of the three centres occur in the regions of the other (beside the North Atlantic low-pressure zone) prominent SLP systems of the Northern Hemisphere: over the Azores high; the Siberian high and the Aleutian low. Thus, when SLP is lower in the Lofotes area than in the Irminger Sea area of the North Atlantic low-pressure zone, the Azores high is weaker, the Siberian high stronger and the Aleutian low deeper.

The ILD pattern explains 8% of the SLP variability in the area north of 30°N and 13% in the Atlantic sector (60°W–90°E, 40°N–90° N). For comparison, the NAO explains 29% and 36% of the SLP variability, respectively, in the mentioned areas. The explained variance (EV) was calculated as

$$\mathrm{EV} = \sum_{k=1}^{N} \left(p_{\mathrm{ILD}}^{\mathrm{norm}}(i,j)\Delta p_k(i,j)\right)^2 \Big/ \sum_{k=1}^{N} (\Delta p_k(\mathrm{i},\mathrm{j})\Delta p_k(i,j)). \tag{3}$$

In (3), $\Delta\ p_k(i,j)$ is the latitude (i)–longitude (j) pressure anomaly field for month k ($k = 1 \ldots N$; $N = 135$) and $p_{\mathrm{ILD}}^{\mathrm{norm}}\ (i,j)$ the ILD pressure field (Fig. 5) normalized by its standard deviation.

The ILD pattern is statistically significant at the 5% level. The significance was calculated using a two-tailed t-test as follows. The 19 cases with ILD index $> +\sigma$ (I cases) and the 20 cases with ILD index $< -\sigma$ (L cases), resulting in 380 pairs, are used to calculate the corresponding L minus I pressure difference fields, on which the t-test is applied.

The ILD index time-series for each winter month, December, January and February, of the 45-year-long ERA-40 period is presented in Fig. 6. The winter ILD index varies between +4.5 and –3.5 and shows variations on intraseasonal, interannual and decadal timescales. For comparison, the NAO index (NCAR, 2007) based on the difference of normalized SLP among the stations Lisbon, Portugal and Stykkisholmur, Iceland, is also shown in Fig. 6. The correlation coefficient between ILD and NAO index is 0.25 for the winter months (DJF). The correlation between ILD index and NAO index appears to change around the year 1976. The correlation for the first (1957–1976) and second (1977–2002) time period is 0.45 and 0.09, respectively. For about the same time, Hilmer and Jung (2000) find a change in the correlation between NAO and Fram Strait ice export. Lu and Greatbatch (2002) analyse a change in the relationship between NAO and Northern Hemisphere climate variability occurring around the same year.

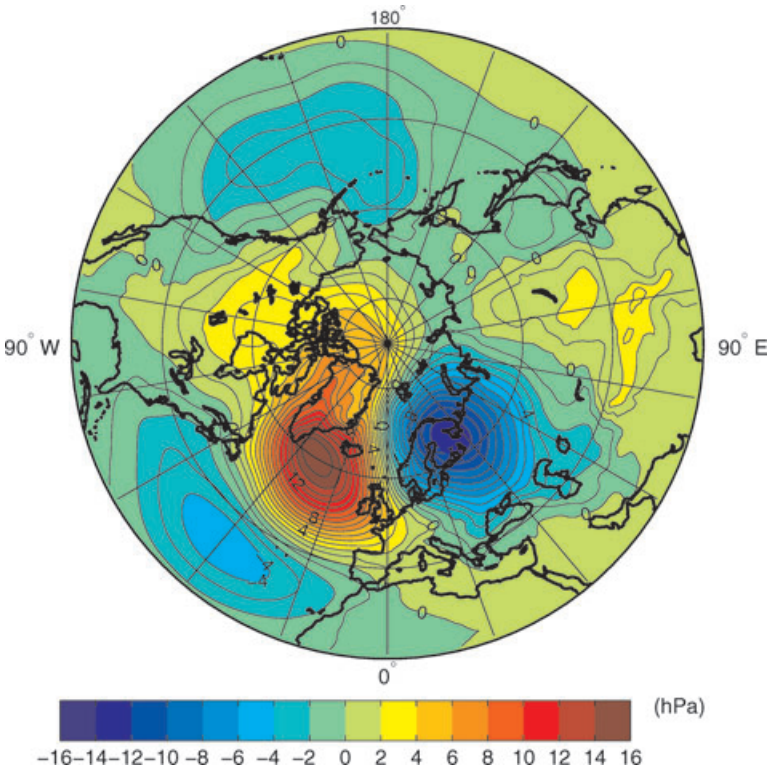

Fig. 5. ILD pattern: SLP difference field for low ($< -\sigma$) minus high ($> +\sigma$) ILD index for winter months (D, J, F) 1957–2002.

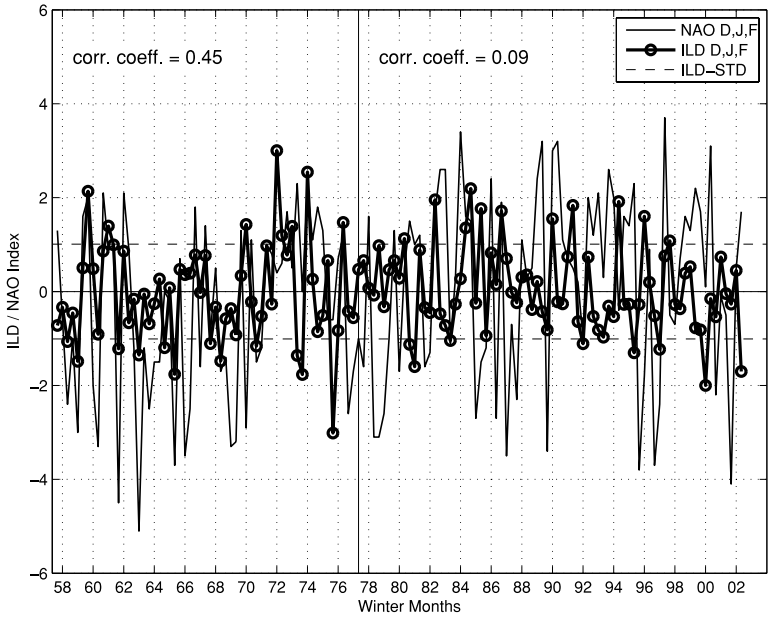

Fig. 6. ILD and NAO index for individual winter months (D, J, F) for 1957–2002, with correlation coefficients for the first (1957–1976) and second (1977–2002) time period.

The ILD pattern extends throughout the troposphere and even into the stratosphere. This is shown in Fig. 7 by the geopotential height (GPH) difference patterns at the 1000, 850, 500, 250, 100 and 50 hPa levels. Whereas the two primary ILD centres (Iceland, Lofotes) are present at all levels, the relative importance of the three secondary centres changes with height. Particularly striking is that the amplitude of the GPH variations over the Siberian high region is continuously increasing with height. The Aleutian low weakens and a new low appears in the Bering Strait in the stratosphere. The importance of the Azores high vanishes with height so that the ILD pattern changes from five centres at sea level to four centres at 50 hPa.

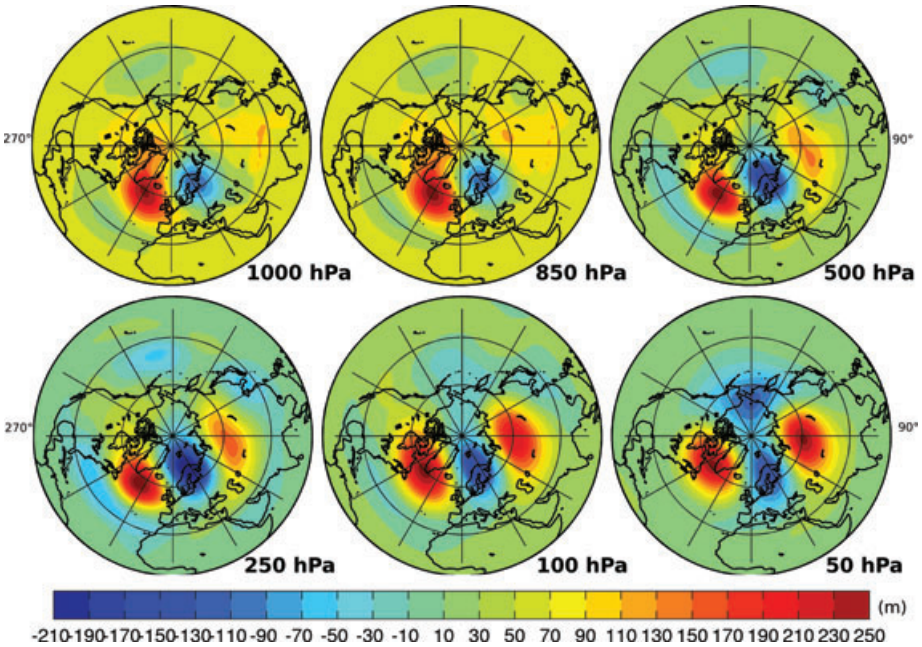

Fig. 7. ILD pattern with height: geopotential height difference fields at 1000, 850, 500, 250, 100 and 50 hPa for low ($< -\sigma$) minus high ($> +\sigma$) ILD index for winter months (D, J, F) 1957–2002.

4. Relation of ILD pattern to air temperature, Arctic sea ice concentration and ice export through Fram Strait

The ILD pattern (Fig. 5) within the North Atlantic low-pressure zone causes changes of the meridional wind component. To which extend these changes impact the surface SAT field over the North Atlantic region and the Arctic sea ice conditions is investigated below.

The SAT difference field between the 20 cases with low (less than –1 standard deviation) and the 19 cases with high (more than +1 standard deviation) ILD index is presented in Fig. 8. The highest impact on SAT is found for the northeastern North Atlantic (Nordic Seas), with up to –7 K difference. Also at the outside edges of the two primary ILD centres, SAT differences with opposite sign are remarkable, for example, up to +5 K over Labrador Sea and Middle Asia. Our findings over Middle Asia are in agreement with the study of Rogers and Mosley-Thompson (1995), who also found that warm or cold winters in Siberia are connected with the occurrence or absence of a second low over the Norwegian Sea (their figs 2 and 4). A similar SAT anomaly distribution over the Nordic Seas and Labrador Sea, as found in this paper, was obtained by Wu et al. (2004) from composites of heavy and light Arctic ice winters. This suggests that the ILD index may be a suitable parameter to characterize also Arctic sea ice conditions.

We look at the relation between ILD pattern and Arctic sea ice in more detail. For this purpose, we use the data sets of sea ice concentration from the ERA-40 re-analysis and ice motion from the US National Sea Ice Data Center (Fowler, 2003, updated 2007). The ice concentration difference field between low minus high ILD index winter months in Fig. 9 shows the largest positive differences of ice concentration in a stripe from Svalbard to the southeast coast of Greenland and large negative differences in Labrador Sea and Baltic Sea. All these differences fit well with the wind directions inferred from the ILD pattern (Fig. 5) and with the corresponding SAT difference pattern (Fig. 8).

Monthly means of sea ice motion for the winter months (DJF) are available only for the period 1979–2002, which is about half of the ERA-40 period. The ice motion is given as u and v components in a Cartesian coordinate system, with its positive u axis pointing from the North Pole to 90°E and its positive v axis pointing from the North Pole toward 180°E. The ice motion difference fields between low and high ILD index winter months are shown in Fig. 10. The largest negative differences of the u and v component of ice motion occur in the region north of Franz Joseph Land and Svalbard, in the Fram Strait and along the East Greenland current. The ice motion differences fit well with the ILD pattern in Fig. 5. In the Fram Strait, between 79°N and 80°N, (where the v component alone represents approximately the total ice motion), the absolutely largest v differences of –0.04 m s^{-1} occur. This difference implies that the ILD pattern affects the Fram Strait sea ice export by ±20% of its mean value (mean v component approximately –0.11 ms^{-1}). A comparably large amplitude holds also for the interannual variability of the annual Fram Strait sea ice export (e.g. Hilmer et al., 1998; Kwok and Rothrock, 1999; Vinje, 2001). The correlation between the ILD index and the v component of ice motion averaged between 79°N and 80°N in Fram Strait amounts to 0.43.

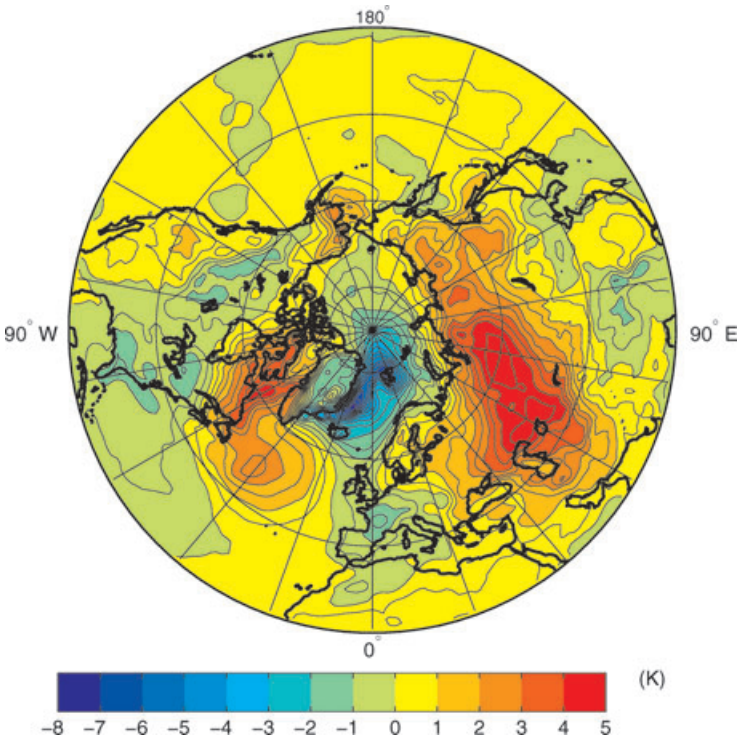

Fig. 8. Difference of surface air temperature (SAT) for low ($< -\sigma$) minus high ($> +\sigma$) ILD index for winter months (D, J, F) 1957–2002.

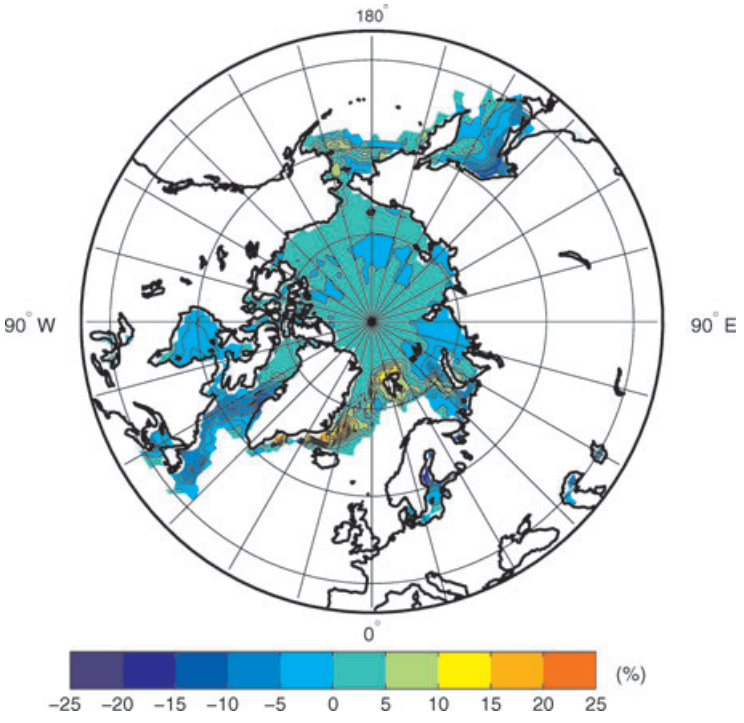

Fig. 9. Difference of sea ice concentration for low ($<-\sigma$) minus high ($> +\sigma$) ILD index for winter months (D, J, F) 1957–2002.

5. Summary and discussion

The North Atlantic low-pressure zone is the dominating SLP pattern over the northeast Atlantic. Two low-pressure centres occur within the elongated zone in the long-term winter mean: the primary one over Irminger Sea near Iceland and the secondary one off the coast of Norwegian Lofotes Islands. In monthly mean SLP fields during wintertime, the secondary low-pressure centre shows up in about two thirds of the time. This high frequency of the second low-pressure centre together with the existence of

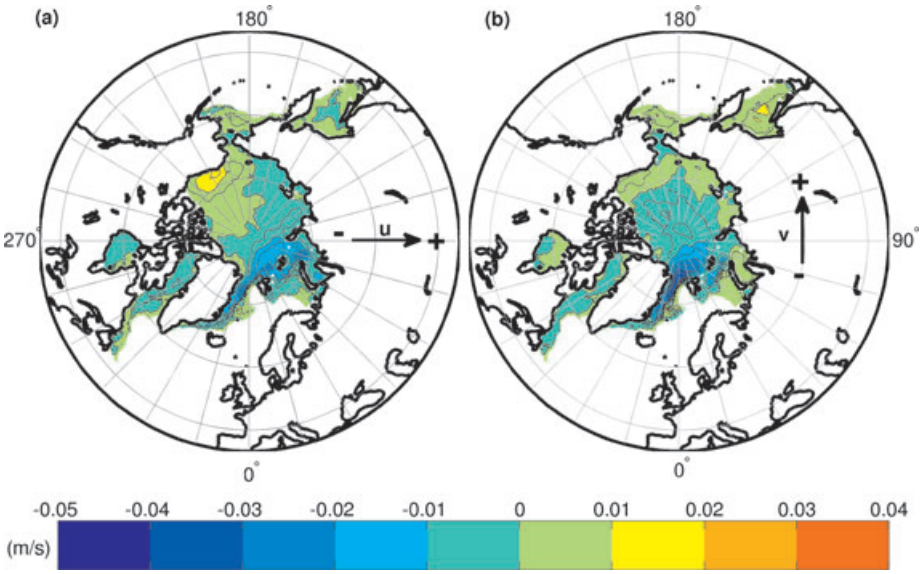

Fig. 10. Difference of u component (a) and v component (b) of sea ice motion for low ($< -\sigma$) minus high ($> +\sigma$) ILD index for winter months (D, J, F) 1957–2002. Ice data are from Fowler (2003, updated 2007).

a secondary frequency maximum of cyclone occurrence along the coast of North Norway motivated us to investigate the variability of the pressure distribution within the North Atlantic low-pressure zone in more detail.

Based on the pressure anomalies at both centres (Irminger Sea, Lofotes), the states of co- and antivariability were investigated. The covariability represents states of a strongly or weakly developed North Atlantic low-pressure zone. The difference pattern of the composite SLP fields for these two states represents the NAO pattern. The antivariability represents states with opposite signs of the pressure anomaly at both centres. To describe the antivariability independent of the general pressure level of the North Atlantic low-pressure zone, an ILD index was defined, which is positive (negative) when the anomaly in the Lofotes area is higher (lower) than that in the Irminger Sea area.

An ILD pattern was calculated as difference between SLP composites for high and low values of the ILD index. The ILD pattern extends horizontally beyond the two centres and affects other prominent Northern Hemispheric pressure centres: Aleutian low; Siberian high and Azores high. The pattern extends throughout the troposphere, into the stratosphere. The ILD pattern shows significant impacts on SAT, Arctic ice concentration and ice motion. It is noticeable that the pressure anomalies in the Irminger Sea and Lofotes area are suited to describe the west-east as well as the north-south pressure variability over the North Atlantic.

The SLP variability at high latitudes of the Northern Hemisphere but not focused on the North Atlantic low-pressure zone, was studied by Skeie (2000), Cavalieri and Häkkinen (2001) and Wu et al. (2006). Skeie (2000) applied EOF methods and found an exceptional SLP pattern anomaly in the second EOF (his Fig. 1b), with its centre over the southeastern Barents Sea, which resembles the northeastern centre of the ILD pattern in Fig. 6. Furthermore, the second EOF even shows a counterpart with similar shape over the area of the southwestern centre of the ILD pattern. Skeie referred to the variation of the second EOF as the Barents Sea oscillation (BSO) and found a close relation between the BSO and the Fram Strait sea ice export.

Confining the EOF analysis of SLP to the area north of 70°N in contrast to Skeie (2000), who studied the area north of 30°N, Wu et al. (2006) found a dipole-like SLP anomaly in the second EOF over the Arctic, with its centres over the Kara Sea and the Canadian archipelago. Although the second EOF explains only 13% of the Arctic SLP variability, the dipole anomaly is well related to the Arctic sea ice motion and Fram Strait ice export.

Cavalieri and Häkkinen (2001) found a close connection between the Fram Strait ice export and the phase positions of wavenumber 1 and 2 circumpolar waves. Their SLP composites for cases with negative and positive differences of the wave 1 and wave 2 phase positions from the average position (their fig. 3) show remarkable similarities to the two opposite ILD states, with either only one SLP minimum over the Irminger Sea or two minima, where the other minimum is located over the Norwegian/ Barents Sea region. The correlation between the phase location of wave 2 (for the 45 January months between 1958–2002 taken from fig. 1a in Cavalieri and Häkkinen, 2001) and the ILD index amounts to –0.5. Cavalieri and Häkkinen (2001) state that the two SLP composite patterns, although they share some of the features of the NAO pressure anomalies at the low and high index phase, 'clearly represent a separate dynamical entity due to the low pressure anomaly extending to the Barents Sea.'

The question arises if the ILD is an east-west shift of the NAO centres. Many papers deal with the west-east shift of the

NAO centres, for example, under increased CO_2 concentration (Ulbrich and Christoph, 1999), under increased background westerlies (Lou and Gong, 2006), as the effect of non-linear dynamics (Petersen et al., 2003) or deal simply with the motion of the Icelandic low position (Mächel et al., 1998). However, these papers do not address explicitly the fact of the existence of a second minimum in the elongated North Atlantic low-pressure zone. Our analysis indicates that the variation of the pressure difference in the low-pressure zone is not simply a west-east shift of the NAO centres. In that case, a further SLP dipole in the ILD pattern should occur at the eastern side of the Azores high area, which is not the case.

This paper as well as the papers of Skeie (2000) and Cavalieri and Häkkinen (2001) show that the SLP variability over the North Atlantic is not sufficiently described by the NAO alone. In addition to the NAO represented by the north-south pressure gradient between Iceland and Azores or the first EOF of the pressure field, the west-east pressure gradient must be regarded. This west-east pressure gradient may be simply described by the ILD index.

A question for further research arises concerning the causes of the ILD variability. In this respect, there are two noticeable results: the relation with the Siberian high and the extension to the stratosphere. The potential of the Siberian high to influence the circulation of the Northern Hemisphere in winter was shown by Cohen et al. (2001). The development of a strong or weak Siberian high is closely connected with the onset of a snow-covered surface in Middle Asia. An earlier onset of snow cover causes a stronger Siberian high. Baldwin and Dunkerton (1999) showed that initial signals of variations of the Arctic oscillation start in the stratosphere, propagate downwards and reach, after a time period of about 90 d, the lower troposphere. Stratosphere–troposphere interactions are affecting NAO variability as studied by Ambaum and Hoskins (2002). It would be interesting to investigate if there is such a precursor for the ILD pattern. However, the time resolution (one month averages), which we have used here, is too coarse to study ILD pattern life cycles. On the basis of monthly averaged SLP fields, the autocorrelation of the ILD index drops to a value of 0.12, already after a time step of one month. Further investigations with a higher time resolution are necessary.

Acknowledgments

This paper was supported by the German Science Foundation (DFG) under grant 'SFB512: Cyclones and the North Atlantic climate system' established at the University of Hamburg, Germany. We thank the anonymous reviewers for their constructive comments.

References

Affeld, B. 2003. *Zyklonen in der Arktis und ihre Bedeutung für den Eisexport durch die Framstraße*. PhD Thesis. Univ. Fachbereich Geowissenschaften, 124 pp, available at: http://www.sub.uni-hamburg.de/opus/volltexte/2003/1009.

Ambaum, M. and Hoskins, B. 2002. The NAO troposphere-stratosphere connection. *J. Clim.* **15**, 1969–1978.

Ambaum, M., Hoskins, B. and Stephenson, D. 2001. Arctic oscillation or North Atlantic oscillation? *J. Clim.* **14**, 3495–3507.

Baldwin, M. and Dunkerton, T. 1999. Propagation of the Arctic oscillation from the stratosphere to the troposphere. *J. Geophys. Res.* **104**, 30 937–30 946.

Cavalieri, D. and S. Häkkinen. 2001. Arctic climate and atmospheric planetary waves. *Geophys. Res. Lett.* **28**, 791–794.

Cohen, J., Saito, K. and Entekhabi, D. 2001. The role of the Siberian high in northern hemisphere climate variability. *Geophys. Res. Lett.*, **28**, 299–302.

Fowler, C. 2003, updated 2007. *Polar Pathfinder Daily 25 km EASE-grid Sea Ice Motion Vectors*. National Sea Ice Data Center (NSIDC), Boulder, CO. Available at: http://nsidc.org/data/docs/daac/nsidc0116_icemotion.gd.html.

Hilmer, M. and Jung, T. 2000. Evidence for a recent change in the link between the North Atlantic oscillation and Arctic Sea ice export. *Geophys. Res. Lett.* **27**, 989–992.

Hilmer, M., Harder, M. and Lemke, P. 1998. Sea ice transport: a highly variable link between Arctic and North Atlantic. *Geophys. Res. Lett.* **25**, 3359–3362.

Hurrell, J. W. 1995. Decadal trends in the North Atlantic oscillation: regional temperatures and precipitation. *Science* **269**, 676–679.

Hurrell, J. W., Kushnir, Y., Ottersen, G. and Visbeck, M. (eds.) 2003. An overview of the North Atlantic oscillation. In: *The North Atlantic Oscillation, Geophysical Monograph* Volume 134. AGU, 1–34.

Jones, P. D., Jonsson, T. and Wheeler, D. 1997. Extension of the North Atlantic oscillation using early instrumental pressure observations from Gibraltar and Southwest Iceland. *Int. J. Climatol.* **17**, 1433–1450.

Kwok, R. and Rothrock, D. A. 1999. Variability of Fram Strait ice flux and North Atlantic oscillation. *J. Geophys. Res.*, **104**, 5177–5189.

Lu, J. and Greatbatch, R. J. 2002. The changing relationship between the NAO and northern hemisphere climate variability. *Geophys. Res. Lett.* **29**, 1148, doi:10.1029/2001GL014052.

Luo, D. and Gong, T. 2006. A possible mechanism for the eastward shift of interannual NAO action centers in last three decades. *Geophys. Res. Lett.* **33**, L24815, doi:10.1029/2006GL027860.

Mächel, H., Kapala, A. and Flohn, H. 1998. Behaviour of the centers of action above the atlantic since 1881. Part I: characteristics of seasonal and interannual variability. *Int. J. Climatol.* **18**, 1–22.

NCAR (National Center for Atmospheric Research). 2007. NAO index data provided by the Climate Analysis Section, NCAR, Boulder, USA (Hurrell 1995). Available at: http://www.cgd.ucar.edu/cas/jhurrell/indices.html.

Peterson, K. A., Lu, J. and Greatbatch, R. J. 2003. Evidence of nonlinear dynamics in the eastward shift of the NAO. *Geophys. Res. Lett.* **30**, 1030, doi:10.1029/2002GL015585.

Rogers, J. C. 1997. North Atlantic storm track variability and its association to the North Atlantic oscillation and climate variability of Northern Europe. *J. Clim.* **10**, 1635–1647.

Rogers, J. C. and Mosley-Thompson, E. 1995. Atlantic Arctic cyclones and the mild Siberian winters of the 1980s. *Geophys. Res. Lett.* **22**, 799–802.

Serreze, M. C., Carse, F., Barry, R. and Rogers, J. 1997. Icelandic low cyclone activity: climatological features, linkages with the NAO, and relationships with recent changes in the Northern Hemisphere circulation. *J. Clim.* **10**, 453–464.

Skeie, P. 2000. Meridional flow variability over the Nordic Seas in the Arctic oscillation framework. *Geophys. Res. Lett.* **27**, 2569–2572.

Ulbrich, U. and Christoph, M. 1999. A shift of the NAO and increasing storm track activity over Europe due to anthropogenic greenhouse gas forcing. *Clim. Dyn.* **15**, 551–559.

Uppala, S. M., Kållberg, P. W., Simmons, A. J., Andrae, U., da Costa Bechtold, V. and co-authors. 2005. The ERA-40 re-analysis. *Q. J. R. Meteorol. Soc.* **131**, 2961–3012.

Vinje, T. 2001. Fram Strait ice fluxes and atmospheric circulation: 1950–2000. *J. Clim.* **14**(16), 3508–3517.

Wallace, J. M. 2000. North Atlantic oscillation/annular mode: two paradigms—one phenomenon. *Q. J. R. Meteorol. Soc.* **126**, 791–805.

Wernli, H. and Schwierz, C. 2006. Surface cyclones in the ERA-40 dataset (1958–2001). Part I: novel identification method and global climatology. *J. Atmos. Sci.* **63**, 2486–2507.

Wu, B., Wang, J. and Walsh, J. 2004. Possible feedback of winter sea ice in the Greenland and Barents Sea on the local atmosphere. *Mon. Wea. Rev.* **132**, 1868–1876.

Wu, B., Wang, J. and Walsh, J. 2006. Dipole anomaly in the winter Arctic atmosphere and its association with sea ice motion. *J. Clim.* **19**, 210–225.